

Coherent amplitudon generation in $\text{K}_{0.3}\text{MoO}_3$ through ultrafast inter-band quasi particle decay

D. M. Sagar,¹ A. A. Tsvetkov,¹ D. Fausti,¹ S. van Smaalen,² and P. H. M. van Loosdrecht^{1,*}

¹*Material Science Center, University of Groningen,
9747 AG Groningen, The Netherlands.*

²*Laboratory of Crystallography, University of Bayreuth, 95440 Bayreuth, Germany.*

(Dated: April 10, 2018)

Abstract

The charge density wave system $\text{K}_{0.3}\text{MoO}_3$ has been studied using variable energy pump-probe spectroscopy, ellipsometry, and inelastic light scattering. The observed transient reflectivity response exhibits quite a complex behavior, containing contributions due to quasi particle excitations, coherent amplitudons and phonons, and heating effects. The generation of coherent amplitudons is discussed in terms of relaxation of photo-excited quasi particles, and is found to be resonant with the interband plasmon frequency. Two additional coherent excitations observed in the transients are assigned to zone-folding modes of the charge density wave state.

PACS numbers: 78.47.+p, 73.20.Mf, 71.45.Lr, 78.67.-n, 78.30.-j

I. INTRODUCTION

A Charge density wave transition is a metal to insulator transition originating from the inherent instability of a one dimensional charge system coupled to a three dimensional lattice^{1,2,3,4}. Due to the electron-phonon coupling the electron density condenses in a charge modulated state (modulation wavelength $\lambda = \pi/k_F$, with k_F the Fermi wavevector), and a charge density wave gap opens in the single particle excitation spectrum at the Fermi energy. Above a certain temperature (the Peierls temperature T_p) these materials are quasi one dimensional metals, below T_p they are either insulators or semi-metals. Charge density wave systems exhibit a number of intriguing phenomena, ranging from Luttinger liquid like behavior in the metallic state⁵ to highly non-linear conduction and quasi periodic conductance oscillations in the charge ordered state^{4,6}. The non-linear conduction seems to be a property which is not unique to charge density wave systems, as it is observed in other low dimensional charge ordering systems as well⁷. One of the well known inorganic systems exhibiting charge density wave transitions are the blue bronzes⁸. The term bronze is applied to a variety of crystalline phases of the transition metal oxides. They have a common formula $A_{0.3}MoO_3$, where the alkali metal A can be K, Rb, or Tl, and are often referred to as *blue* bronzes because of their deep blue color. The crystal structure of blue bronze contains rigid units comprised of clusters of ten distorted MoO_6 octahedra, sharing corners along the monoclinic b-axis⁹. This corner sharing provides an easy path for the conduction electrons along the [102] directions. The band filling is $3/4^3$. The particular material addressed in this paper is $K_{0.3}MoO_3$ which is a quasi-one-dimensional metal which undergoes the metal to insulator transition ($T_{CDW} = 183$ K) through the Peierls channel.^{9,10}

Apart from the usual single particle excitations (quasi particles), charge density wave systems possess two other fundamental excitations, which are of a collective nature. They arise from the modulation of the charge density $\rho(r) = \rho_0 + \rho_1 \cos(2k_F r + \phi)$, and are called phasons and amplitudons for collective phase (ϕ) and amplitude (ρ_1) oscillations, respectively. Ideally, the phason is the gapless Goldstone mode, leading to the notion of Fröhlich superconductivity¹¹. However, due to the electrostatic interactions of the charges with the underlying lattice and possibly with impurities and imperfections, the translational symmetry of the state is broken leading to a finite gap in the phason dispersion spectrum. In contrast the amplitudon has an intrinsic gap in its excitation spectrum¹². In centrosym-

metric media the phason has a *ungerade* symmetry, and is therefore infrared active, and the amplitudon mode (AM) has a *gerade* symmetry and hence Raman active^{3,13}. The phason mode is relatively well studied by for instance neutron scattering^{14,15} and far infrared spectroscopy^{3,13}, and plays an important role in the charge density wave transport. The amplitudon, *i.e.* the transverse oscillation of the coupled charge-lattice system, has been observed experimentally in for instance Raman experiments⁹. Transient experiments have proven to be versatile tools in studies on the properties of CDW materials as well. Optically induced transient oscillatory conductivity experiments have shown that one can increase the coherence length of the CDW correlations by exciting quasi particles from the CDW condensate¹⁶. An important breakthrough was the observation that one can coherently excite the amplitudon mode in pump-probe spectroscopy experiments^{17,18,19}. These experiments open the possibility to study the temporal dynamics of the collective and single particle charge density wave excitations, as well as their interactions with quasi particles and vibrational excitations. Demsar *et al.*,¹⁷ observed the amplitudon in $\text{K}_{0.3}\text{MoO}_3$ as a real-time coherent modulation of the transient reflectivity with the frequency of the amplitudon mode. The frequency and the decay time of the AM oscillation was measured as 1.67 THz and 10 ps, respectively. It was also found that the single particle excitations across the CDW gap appear as a rapidly decaying contribution to the transient reflectivity. The mechanism of the coherent AM generation was speculated to be Displacive Excitation of Coherent Phonons (DECP²⁰) which is the mechanism which describes the generation of coherent phonons in absorbing media^{21,22,23}. The experiment was performed with the pump and the probe wavelength fixed at 800 nm and at a low pump fluency of $1 \mu\text{J}/\text{cm}^2$. The aim of the present study is to obtain a better understanding of the transient response of the charge density wave material $\text{K}_{0.3}\text{MoO}_3$, and more in particular of the generation and dephasing mechanisms of coherent amplitudon oscillations. These issues are addressed using variable energy pump-probe spectroscopy, ellipsometry and Raman scattering experiments.

II. EXPERIMENTAL

A regenerative Ti:Sapphire amplifier seeded by a mode-locked Ti:Sapphire laser was used to generate laser pulses at 800 nm with a temporal width of 150 fs, operating at 1 kHz repetition rate. The relatively low repetition rate minimizes heating effects due to the pile-

up of the pulses. To obtain laser pulses of continuously tunable energies a Traveling Wave Optical Parametric Amplifier of Superfluorescence (TOPAS) was used. The TOPAS contains a series of nonlinear crystals based on ultrashort pulse parametric frequency converters that allows for a continuous tuning over a wide wavelength range. The output of TOPAS is used as the pump-pulse and the wavelength of the probe is kept at 800 nm through out the experiment. The pump and the probe were focused to a spot of 100 microns and 50 microns diameter respectively. In the wavelength dependent measurements the pump-fluency was kept constant and in the pump-fluency-dependent measurement the wavelength of the pump was kept constant. The polarization of the incident pump pulse was parallel to the b-axis along which the charge density wave ordering develops. The experiments are performed in a reflection geometry with the angle of the pump and probe pulses close to normal incidence with respect to the sample surface. The sample was placed in a He-flow cryostat, which allows to vary the temperature between 4.2 and 300 K (stability ± 0.1 K). Raman experiments have been performed using a standard triple grating spectrometer, using 532 nm excitation. The ellipsometry experiments have been performed using a Woollam spectroscopic ellipsometer with the sample placed in a special home build UHV optical cryostat.

III. TRANSIENT REFLECTIVITY

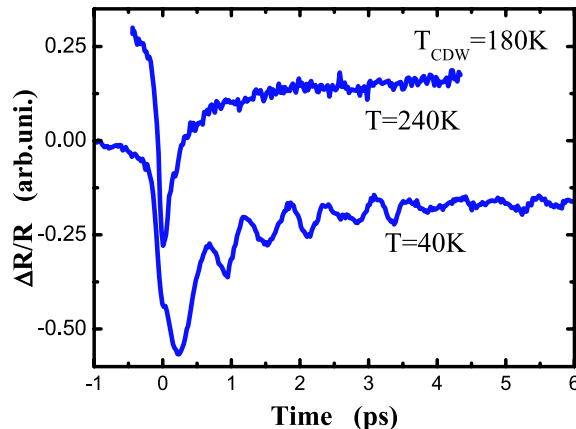


FIG. 1: The transient reflectivity response of $K_{0.3}MoO_3$ above and below T_{CDW} .

The formation of the charge density wave in blue bronze leads to drastic changes in the nature the transient reflectivity. This is exemplified in Fig.1 which shows two representative transient reflectivity traces recorded above and below T_{CDW} obtained using 800 nm for both

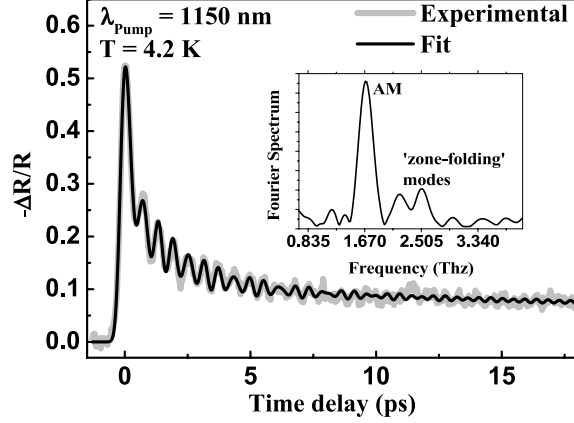


FIG. 2: The transient reflectivity response of $\text{K}_{0.3}\text{MoO}_3$ at $T = 4.2$ K, using a 1150 nm pump pulse (grey line). The dark line represents a fit of Eq. 1 to the data. *Inset:* Fourier spectrum showing the amplitudon mode at 1.67 THz, and two zone folded phonons at 2.25 THz and 2.5 THz.

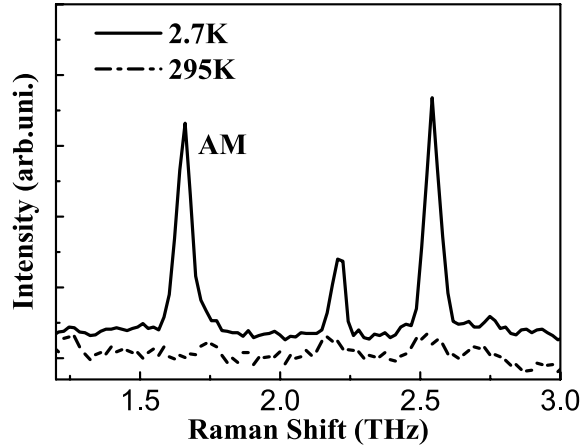


FIG. 3: The (bb) polarized raman spectrum of $\text{K}_{0.3}\text{MoO}_3$ above and below the CDW transition temperature, showing the appearance of the amplitudon mode and the two fully symmetric modes.

the pump and the probe wavelengths. Above the phase transition ($T = 240$ K curve) the material is metallic and gapless leading to a featureless very fast decay (faster than the time resolution 150 fs) of the excited electrons, followed by a slower decay which may be attributed to electron-phonon coupling induced heating effects. In the charge density wave state (Fig. 1 $T = 40$ K curve, and Fig 2) the response is more interesting due to the presence of various coherent excitations and a slowing down of the decay of the excited quasi particles resulting from the opening of the CDW gap in the electronic excitation spectrum. A Fourier analysis of the response (see inset Fig. 2) shows the presence of three coherent excitations.

The strongest component found at 1.67 THz has been attributed to the coherent excitation of the collective amplitudon mode¹⁷. The two additional modes at 2.25 and 2.5 THz can be attributed to Raman active phonons which are activated in the CDW state due to folding of the Brillouin zone¹⁰. Polarized frequency domain Raman scattering experiments have indeed confirmed this interpretation (see Fig. 3). The excitation wavelength for this experiment was 532 nm with the polarization of the incoming and scattered light parallel to the b-axis of the crystal. Above the phase transition temperature ($T = 295$ K spectrum) the Raman spectrum is rather featureless in the region of the amplitudon mode. In contrast, the 2.7 K spectrum shows the appearance of just the three modes which are also observed in the time domain traces.

The electronic contribution to $\Delta R/R$ can be discussed in terms of their relaxation time scales. Since the energy of the pump pulse is much larger than the CDW gap ($\Delta_{CDW}=0.12$ eV¹³) one expects that the optical pumping excites a large number of quasi particles ($\frac{E_{Pump}}{\Delta} \sim 30-50$ QP's per photon) across the CDW-gap. After this photo excitation a very fast internal thermalization of the highly non-equilibrium electron distribution occurs on a time scale of a few fs, which is followed by electron-phonon thermalization that occurs on a time scale less than 100 fs¹⁷. Although the temporal resolution of the current experiments is not enough to observe these effects, once the quasi particles have internally thermalized and relaxed to states near the Fermi level, further energy relaxation is delayed due to the presence of the CDW-gap. The presence of the CDW-gap acts as a "bottle-neck" for the thermalized quasi particles^{24,25}. The typical time for relaxation over the CDW gap is found to be 0.6 ps in the present experiments. However, the observed decay is not a simple exponential but it is rather a stretched exponential decay which is typical for a system with a distribution of relaxation times as is for instance found in systems with an anisotropic gap such as 1T-TaS₂¹⁸. Even though blue bronze is only quasi-one dimensional, there is no evidence for an anisotropic gap in this system. It is more likely that the stretched decay originates from distribution of relaxation times resulting from a possible glassy nature of the CDW ground state^{24,25}. Finally, like in the high temperature phase, a long time relaxation of $\Delta R/R$ is observed, which may be attributed to heating effects. No qualitative difference with the high temperature relaxation is observed here, ruling out a possible contribution of phasons to the response as has been suggested earlier¹⁷.

To summarize, the observed transient reflectivity response in the CDW phase can be

described by

$$\frac{\Delta R}{R} = Ae^{(-t/\tau_{QP})^n} + \sum_j A_j e^{-t/\tau_j} \cos(\omega_j t) + Be^{-t/\tau_L} \quad , \quad (1)$$

where the first term describes the quasi particle response using a stretched exponential decay with time constant τ_{QP} and stretch index n which takes the relaxation of the quasi particles across the CDW gap into account. The second term in this expression accounts for the observed coherent amplitudon and phonon oscillations with frequencies ω_j and decay times τ_j , and the last term represents the observed long time response with a decay time τ_L presumably originating from heating effects.

A fit of Eq. 1 to the data generally leads to excellent agreement with the data, as is for instance shown in Fig. 2. For this fit the quasi particle decay time is found to be $\tau_{QP} = 0.65$ ps with $n = 1/2$, and the amplitudon lifetime $\tau_{AM} = 3.5$ ps. The decay times of the two coherent phonons is of the order of 20 ± 5 ps, whereas the cooling time is too slow to determine with any accuracy ($\tau_L > 60$ ps). It is interesting to note that the coherent amplitudon is very short lived when compared to the two coherent phonons. This heavy damping of coherent amplitudon presumably results from amplitudon-quasi particle scattering leading either to a decay or to a dephasing of the coherent amplitudon excitation. The observation that the decay time in the present experiment is shorter than in the experiments by Demsar et al.¹⁷, who reported $\tau_{AM} = 10$ ps is consistent with this. The density of excited quasi particles in the current experiments is substantially higher (several orders of magnitude) than in the previous experiments, leading to this faster decay of the coherent amplitudon mode, and also to a larger magnitude of the induced response (here as large as 0.1, compared to 10^{-4} in Ref.¹⁷). The quasi particle lifetime measured for the lowest pump fluency is about 0.6 ps which is close to the value measured by Demsar et al. (0.5 ps)¹⁷. Besides the quasi particle density, the main difference is that the experimental temperature in our case is $T = 4.2$ K whereas in¹⁷ it is $T = 45$ K. The stretched exponential behavior observed in the present study, in contrast to the single exponent in Demsar's study, might be due to the presence of a glassy state which has recently been discussed in literature^{24,25,26}. The stretched exponential behavior is typical for a glassy state.

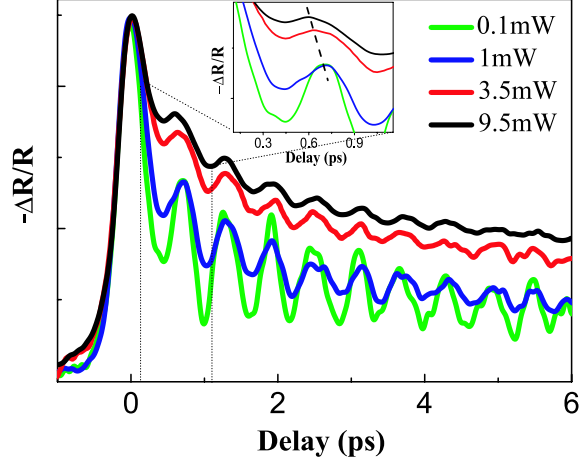


FIG. 4: (Color online) Normalized time resolved reflectivity traces for 800 nm pump-probe experiments with a pump fluency varying between 0.1 and 10 mW. The data is normalized to the zero delay response. The insert shows the position of the first beating of the coherent mode evidencing a phase shift upon increasing fluency.

IV. PUMP FLUENCY DEPENDENCE

In order to address the generation mechanism of the coherent AM pump-fluency dependent (this section) and pump-wavelength (see section V) dependent experiments have been carried out. The experiments reported in Fig. 4 are performed with a relatively high pump fluency of 1-10 mJ/cm². Note that the data are scaled to the strength of the initial response, *i.e.* to the strength of the quasi particle peak. The strength of the quasi particle peak itself is found to be linearly dependent on the pump fluency (see Fig. 5 (b)). This linear dependence is consistent with the expectation that the density of the excited electrons scales with the mean number of photon of the light pulse. Hence, if the generation mechanism of the coherent AM modes can be described, as suggested in²⁷, by the simple theory of displacive excitation (DECP)²⁰, a linear dependence of the coherent excitation amplitude with the pump fluency is expected. On the contrary, Fig.4 and Fig.5(a) clearly show that the intensity of the coherent amplitudon oscillations decreases dramatically with increasing the pump fluency. This immediately rules out the possibility of a linear relationship between the number of photons of the pump pulse and the observed amplitude of the coherent AM mode. A second striking feature of the pump fluency dependence of the time resolved reflectivity traces is the substantial increase in the quasi particle lifetime with the pump power (see

Fig.5(b)).

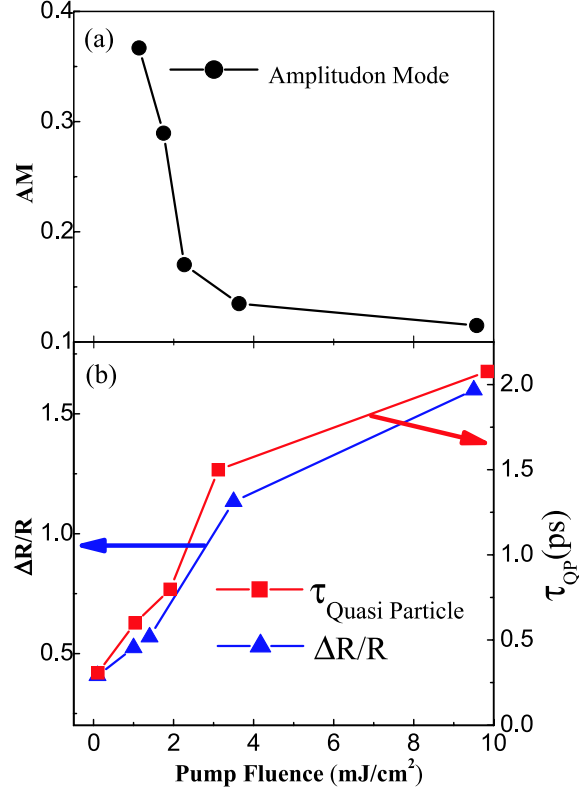


FIG. 5: (Color online) Dependence of the AM amplitude (a), and the quasi particle lifetime and amplitude of the quasi particle peak (b) on the pump fluency. The QP life time and the quasi particle peak show a linear increase with pump fluency, while the AM amplitude shows a dramatic decrease. The solid lines are guides to the eye.

The increasing lifetime of the quasi particles, which is probably due to state filling effects, together with the decreasing amplitudon amplitude seems to indicate that the coherent amplitudons are not directly generated by a coupling to the photons, but rather by a coupling to the decay of the quasi particle excitations. *I.e.* the coherent amplitudon oscillation are generated by the decay processes of the excited electron population. The increasing of the quasi particle lifetime leads to a reduction of the coherence of the amplitudons generated, and thereby to a decrease in the amplitude of the coherent response. In a very simple approach, neglecting the temporal width of the pump-pulse and the stretched exponential behavior of the decay of the quasi particle, one can model the quasi particle response by a simple exponential decay ($e^{-t/\tau_{QP}}/\tau_{QP}$ for $t > 0$), and a linear coupling between the quasi particle decay and the amplitudon generation. The resulting coherent amplitudon response

is then given by:

$$\int_0^\infty \frac{A}{\tau_{QP}} e^{-t'/\tau_{QP}} \cos(\Omega(t+t')) = \frac{A}{1 + \Omega_{AM}^2 \tau_{QP}^2} \cos(\Omega t + \arctan(\Omega \tau_{QP})) \quad (2)$$

where A is the integrated area of the quasi particle peak, Ω is the frequency of the AM mode, and τ_{QP} is the quasi particle lifetime. The product $\Omega_{AM} \tau_{QP}$ plays the role of a decoherence factor. For this special case, the dependence of the size of the coherent amplitudon response on $\Omega_{AM} \tau_{QP}$ is Lorentzian. This is valid as long as the quasi particle response is slower than the temporal pump pulse width. For short quasi particle relaxation times, the quasi particle response becomes more symmetric, leading to an decaying exponential dependence of the coherent signal on $\Omega_{AM} \tau_{QP}$.

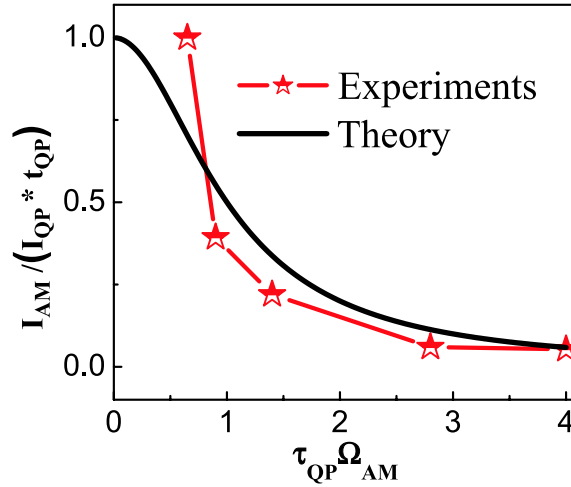


FIG. 6: (Color online) Scaled amplitude (see text) of the coherent AM as a function of the decoherence factor $\tau_{QP} \Omega_{AM}$ (symbols). The decrease with increasing quasi particle life time shows the loss of coherence due to the delayed relaxation of the quasi particles. The solid line displays the amplitude of Eq. 2 as a function of the coherence factor.

To elucidate the point, Fig.6 shows the amplitude of the coherent amplitudon response, normalized to the quasi particle response, as a function of the decoherence factor (symbols). The quasi particle response is approximated as the product of its intensity and lifetime for a given fluency. Inspection of Fig.6 shows that the intensity of the coherent amplitudon decreases rapidly as the decoherence factor reaches unity, beyond which the coherence is lost due to the increase of the quasi particle lifetime and hence dephasing of the generated amplitudons. The same figure also shows the amplitude obtained from Eq.2. Given the

simplicity of the model and the fact that there are no adjustable parameters, the agreement between the experimental data and Eq.2 is rather striking. The small deviation for low decoherence factor is probably due to the assumption of an exponentially decaying quasi particle population. This can be improved by using a more realistic quasi particle response.

In addition to this the decreasing size of the coherent response, the model proposed by (Eq. 2) also predicts a phase shift of the coherent amplitudon response proportional to $\arctan(\Omega_{AM}\tau_{QP})$. This is indeed what is experimentally observed. Comparing just the lowest and the highest fluency (with $\tau_{QP} = 0.3$ and 2.0 ps, respectively), the expected phase shift is $\simeq 2\pi/8$, which is consistent with the experimentally observed shift (see insert Fig. 4).

Some further evidence for the coupling of the photo excited quasi particles to the collective amplitudon mode of the charge density wave state may be found from the pump-wavelength dependent experiments discussed in the next section.

V. THE WAVELENGTH DEPENDENCE

Before discussing the pump-wavelength dependent transient CDW dynamics it is instructive to consider the linear optical response of the system. The linear optical response at various wavelengths provides information on possible absorption bands of the material, eventually giving more insight into the coupling of the electronic transitions with the CDW excitations.

Fig.7 shows the optical response in the wavelength region ranging from 270 nm to 1700 nm. The sharp band in ϵ_2 raising from 500 nm toward the lower wavelength side is due to the "p-d"-transitions involving the electronic excitations from the Oxygen "2p" to the Molybdenum "4d" levels. The quotations are used to indicate that the levels are admixtures rather than pure ones. This is consistent with the photo-emission and electron energy loss experiments done on blue bronze^{28,29}. The broad asymmetric band around 1000 nm is due to interband "d-d"-transitions. The actual zero crossing of ϵ_1 occurs at 1150 nm (1.08 eV). This, however, does not correspond to the actual plasma energy, which occurs at 1.5 eV²⁹. This is also demonstrated in the inset of Fig.7, which shows the energy loss spectrum calculated from the dielectric function. This spectrum shows two peaks, one at the actual plasma frequency (where also a distinct minimum in ϵ_1 is observed), and one at 1.08 eV. This

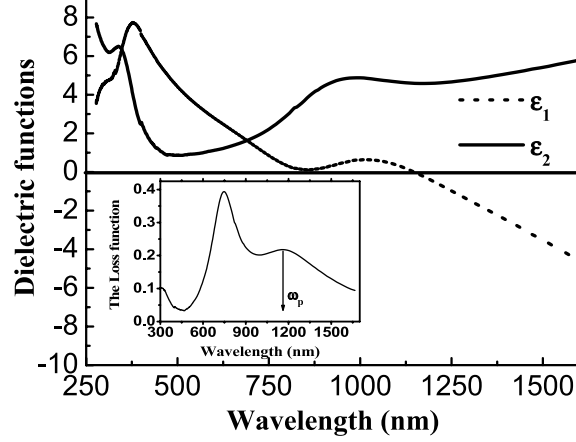


FIG. 7: Optical response ϵ_1 and ϵ_2 of $\text{K}_{0.3}\text{MoO}_3$. *Inset:* The energy loss function calculated from the data in the main panel.

latter energy corresponds to an interband plasmon involving the Mo-d derived dispersionless conduction branch predicted by tight-binding calculations of Travaglini and Wachter^{29,30}.

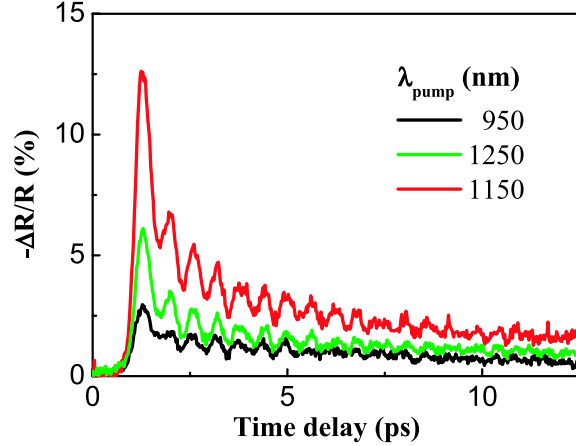


FIG. 8: (Color online) Variation of the transient response with the pump wavelength.

The transient response, and in particular the coherent amplitudon response, depends strongly on the excitation wavelength, and is found to be strongest for $\lambda_{Pump} \sim 1150$ nm and at small wavelengths. This is demonstrated in Fig.8, which shows the transient response for few selected pump wavelengths (λ_{Pump}).

Overall, the amplitude of the coherent amplitudon mode follows the pump energy absorbed in the material. This can be seen from Fig.9, which shows the amplitude of the coherent amplitudon mode measured for various pump wavelengths at a constant pump fluency of 1 mJ/cm^2 . The same graph also shows the amount of absorbed pump energy

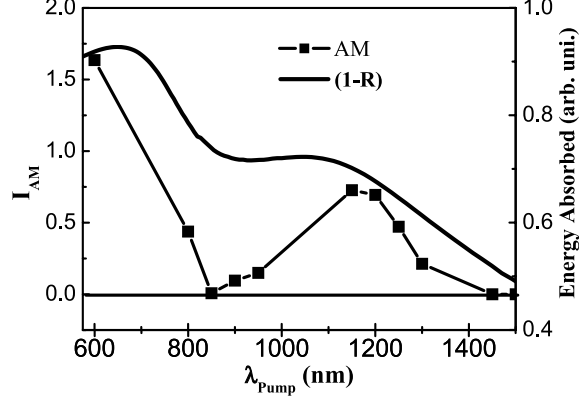


FIG. 9: Coherent amplitudon response as a function of the pump wavelength (symbols, the drawn line is a guide to the eye). The total absorbed pump energy $1-R$, with R the normal incidence reflectivity, is also plotted for comparison (solid line).

calculated from the optical data in Fig.7. It is found that the quasi particle lifetime does not vary strongly with the wavelength. This, together with the fact that the efficiency of the coherent amplitudon generation roughly follows the amount of absorbed energy, and hence the number of photo-excited quasi particles, suggests once again the quasi particle induced nature of the coherent excitation.

Although the coherent AM roughly follows the absorbed energy curve, it does actually not exactly scale with it. In particular, the AM response (as well as the quasi particle response) is markedly peaked near 1150 nm, corresponding to the interband plasma wavelength discussed above. This is surprising since one does not expect the light to couple directly to the plasmon modes (as can also be seen from Fig.7). Nevertheless, the experiments do evidence an efficient coupling most likely through highly excited quasi particles which relax by the emission of plasmon excitations, or through a coupling to surface plasmons. Once excited, the interband plasmons can relax either by emission of lower energy quasi particles which subsequently can excite amplitudons, as the enhanced quasi particle response seems to suggest, or possibly even directly via decay into amplitudon modes.

VI. CONCLUSION

In summary, we studied $\text{K}_{0.3}\text{MoO}_3$ using time resolved spectroscopy, ellipsometry, and polarized Raman spectroscopy. The transient reflectivity experiments show, in addition to

the coherent amplitudon mode observed previously¹⁷, two coherent phonon modes which are also observed in the low temperature Raman spectra. They are assigned to zone-folding modes associated with the charge density wave transition. The lifetime of the coherent amplitudon mode is found to be relatively short, which is believed to be due to the coupling of the AM to the high density of quasi particles.

The generation mechanism of coherent amplitudons in blue bronze does not seem to be the usual DECP²⁰ mechanism, nor the transient stimulated Raman mechanism³¹, since these are not consistent with the observed non linear pump power dependence of the magnitude of the response. It is found that the magnitude of the coherent amplitudon mode depends on the dynamics of the quasi particle decay. It is therefore beleived that the coherent amplitudons are generated through the decay of quasi particles over the Peierls gap. A simple model taking based on this notion accounts well for the observed non linear pump power dependence, as well as for the observed phase shift in the coherent amplitudon response. Pump wavelength dependent experiments, where the coherent amplitudon response is found to be consistent with the equilibrium absorption derived by ellipsometry measurements (and hence with the quasi particle response) further supports the proposed interpretation. The mechanism proposed could be relevant in the generation mechanism of coherent excitations in other highly absorbing materials as well. Further investigations of different compounds are necessary to confirm this.

* Electronic address: P.H.M.van.Loosdrecht@rug.nl

¹ R. E. Peierls, Ann. der Physik **4**, 121 (1930).

² R. E. Peierls, *Quantum theory of solids* (Oxford University Press, Newyork, 1955).

³ G. Grüner, Rev. Mod. Phys. **60**, 1129 (1988).

⁴ G. Grüner, *Density waves in solids* (Addison-Wesley, Reading, MA, 1994).

⁵ F. Wang, J. V. Alvarez, S.-K. Mo, J. W. Allen, G.-H. Gweon, J. He, R. Jin, D. Mandrus, and H. Höchst, Phys. Rev. Lett. **96**, 196403 (2006).

⁶ R. M. Fleming and C. C. Grimes, Phys. Rev. Lett. **42**, 1423 (1979).

⁷ S. Sirbu, P. H. M. van Loosdrecht, T. Yamauchi, and Y. Ueda, Eur. J. Phys. (2006), in press.

⁸ C. Schlenker and J. Dumas, in *Crystal chemistry and Properties of materials with Quasi-One*

- Dimensional Structures.*, edited by J. Rouxel (D. Riedel publishing, Dordrecht, 1986).
- ⁹ G. Travaglini and P. Watcher, Sol. St. Comm. **37**, 599 (1981).
 - ¹⁰ J. P. Pouget, S. Kagoshima, C. Schlenker, and J. Marcus, Phys. Lett **L44**, 113 (1983).
 - ¹¹ H. Frölich, Proc. Royal Soc. London A **223**, 296 (1954).
 - ¹² P. Lee, T. Rice, and P. Anderson, Solid. State. Commun. **14**, 703 (1974).
 - ¹³ L. Degiorgi, B. Alavi, G. Mihály, and G. Grüner, Phys. Rev. B. **44**, 7808 (1991).
 - ¹⁴ C. Escribe-Filippini, J. P. Pouget, B. Hennion, and M. Sato, Synth. Met. **19**, 931 (1987).
 - ¹⁵ B. Hennion, J. P. Pouget, and M. Sato, Phys. Rev. Lett. **68**, 2374 (1992).
 - ¹⁶ P. H. M. van Loosdrecht, B. Beschoten, I. Dotsenko, and S. van Smaalen, J. Phys. IV France **12**, 303 (2002).
 - ¹⁷ J. Demsar, K. Biljakovic, and D. Mihailovic, Phys. Rev. Lett. **83**, 800 (1999).
 - ¹⁸ J. Demsar, L. Forró, H. Berger, and D. Mihailovic, Phys. Rev. B **66**, 041101(R) (2002).
 - ¹⁹ A. A. Tsvetkov, D. M. Sagar, P. H. M. van Loosdrecht, D. van der Marel, and S. van Smaalen, Acta Phys. Pol. B **34**, 387 (2003).
 - ²⁰ H. J. Zeiger, J. Vidal, T. K. Cheng, E. P. Ippen, G. Dresselhaus, and M. S. Dresselhaus, Phys. Rev. B. **45**, 768 (1992).
 - ²¹ F. Vallée and F. Bogani, Phys. Rev. B **43**, 12049 (1991).
 - ²² F. Vallée, Phys. Rev. B. **49**, 2460 (1994).
 - ²³ F. Ganikhanov and F. Vallée, Phys. Rev. B. **55**, 15614 (1997).
 - ²⁴ K. Biljakovic, in *Phase Transitions and Relaxations in Systems with Competing Energy Scales*, edited by T. Riste and D. Sherington (Kluwer Academic, Dordrecht, 1993), p. 339.
 - ²⁵ J. Odin, J. C. Lasjaunias, K. Biljakovic, K. Hasselbach, and P. Monceau, Eur. Phys. J. B **24**, 315 (2001).
 - ²⁶ D. Staresinic, K. Hosseini, W. Brutting, K. Biljakovic, E. Riedel, and S. van Smaalen, Phys. Rev. B. **69**, 113102 (2004).
 - ²⁷ J. Demsar, R. D. Averitt, A. J. Taylor, V. V. Kabanov, W. N. Kang, H. J. Kim, E. M. Choi, and S. I. Lee, Phys. Rev. Lett. **91**, 267002 (2003).
 - ²⁸ G. K. Wertheim, L. F. Schneemeyer, and D. N. E. Buchanan, Phys. Rev. B. **32**, 3568 (1985).
 - ²⁹ M. Sing, V. G. Grigoryan, G. Paasch, M. Knupfer, J. Fink, B. Lommel, and W. Assmus, Phys. Rev. B. **59**, 5414 (1999).
 - ³⁰ G. Travaglini and P. Wachter, in *Charge density waves in Solids.*, edited by G. Hutiray (Springer,

Berlin, 1985), Lecture Notes in Physics, p. 115.

³¹ G. A. Garrett, T. F. Albrecht, J.F. Whitaker, and R. Merlin, Phys. Rev. Lett. **77**, 3661 (1996).